

GAMMA: A General Agent Motion Prediction Model for Autonomous Driving

Yuanfu Luo and Panpan Cai

School of Computing, National University of Singapore,
{yuanfu, caipp}@comp.nus.edu.sg
<https://youtu.be/5xAB0-8XceQ>

Abstract. Autonomous driving in mixed traffic requires reliable motion prediction of nearby *traffic agents* such as pedestrians, bicycles, cars, buses, etc.. This prediction problem is extremely challenging because of the diverse dynamics and geometry of traffic agents, complex road conditions, and intensive interactions between them. In this paper, we proposed GAMMA, a general agent motion prediction model for autonomous driving, that can predict the motion of heterogeneous traffic agents with different kinematics, geometry, etc., and generate multiple hypotheses of trajectories by inferring about human agents' inner states. GAMMA formalizes motion prediction as a geometric optimization problem in the velocity space, and integrates physical constraints and human inner states into this unified framework. Our results show that GAMMA outperforms both traditional and deep learning approaches significantly on diverse real-world datasets.

Keywords: Motion Prediction, Autonomous Driving, Heterogeneous Agents

1 Introduction

Autonomous vehicles navigating in dynamic and interactive environments need to foresee the future motion of nearby *traffic agents* (pedestrians, bicycles, cars, buses, etc.) to ensure safety and efficiency. However, it is extremely challenging to predict the motion of real-world traffic agents, due to the diverse dynamics and geometry of traffic agents, complex road conditions, and intensive interactions between them. We observe that the motion of traffic agents are governed by different *physical constraints* and various *human inner states*. Traffic agents try to reach their destinations under their kinematic constraints, and in the meantime, they share the responsibility for collision avoidance with each other, while having limited attention capabilities.

In this paper, we identify five key factors that govern traffic agents' motions: *kinematics*, *geometry* (collision avoidance), *intention* (destination), *responsibility*, and *attention*. We develop GAMMA, a General Agent Motion prediction Model for Autonomous driving, that integrates these factors in a unified framework. GAMMA formalizes motion prediction as geometric optimization problem in the velocity space, which is conditioned on physical constraints (kinematics

and geometry) and human inner states (intentions, attentions, and responsibilities). The optimization objective of the problem is specified by the intention of a traffic agent, while the constraints are imposed by kinematics, geometry, responsibilities, and attentions.

GAMMA significantly extends the existing geometric optimization framework [1] in the following aspects. First, GAMMA explicitly models heterogeneous kinematics. It enforces the predictions to be kinematically feasible by only considering velocities that can be tracked within a maximum tracking error with the agent’s kinematics. Second, GAMMA uses a polygon representation for traffic agents’ geometry, which is tighter than disc-shaped ones in [1] and much more representative for most real-world traffic agents. Third, GAMMA incorporates various human inner states as part of the model. Since the inner states are hidden and differ from individuals, GAMMA applies Bayesian inference to infer a distribution over possible states for each agent. It then uses the distribution to generate multiple hypotheses of trajectories for the agent.

We compare GAMMA with both geometry-based approaches and deep learning approaches. The comparison is done on two standard benchmark datasets and two new datasets we collected. Results show that GAMMA significantly outperforms both geometry-based and deep learning approaches in predicting real-world trajectories. Our ablation study further demonstrates the importance of the identified key factors in predicting heterogeneous real-world agents.

2 Related Work

In this section, we review the recent motion prediction approaches in two categories: traditional approaches and deep learning approaches.

2.1 Traditional Approaches For Motion Prediction

We categorize the traditional approaches for motion prediction into three groups: social force based, geometric optimization based, and maneuver recognition based approaches. Social force models [2,3,4,5] assume that traffic agents are driven by virtual forces generated from the internal motivations such as reaching the goal, and the external constraints such as avoiding obstacles. Geometric optimization based approaches compute collision-free motions for multiple traffic agents via optimization in the feasible geometric space. The representative work includes Velocity Obstacle (VO) based [6] and the Reciprocal Velocity Obstacle (RVO) based algorithms [7,1,8]. Maneuver recognition based approaches [9,10,11] first classify the traffic agents’ motions into semantically interpretable maneuver using approaches such as HMMs and SVMs, and then predict the motions conditioned on the maneuver with traditional approaches, e.g., polynomial curve fitting, minimization on carefully designed cost functions, etc..

These approaches, however, do not explicitly model the five factors we proposed and hence are not able to handle heterogeneous traffic agents with different kinematics, geometry representations, or human inner states.

Some previous work has considered some of the five factors. NH-ORCA [12] and B-ORCA [13] predict motions considering non-holonomic constraints. AVO [14] takes into account the acceleration constraints to ensure continuous velocity. Those approaches, however, do not generalize to general kinematics, hence cannot handle the interactions between traffic agents with different kinematic constraints. GVO [15] addresses this issue by replacing the geometric formulation of velocity obstacle with a general algebraic representation, which can easily incorporate different kinematics. However, it models poorly the interactions among traffic agents since it assumes all other agents are non-reactive. Some previous work also tried different geometry representations for agents in collision avoidance, such as ellipse [16] and capsule [17]. Ma et al.[18] present a novel CTMAT representation based on medial axis transformation to compute tight bounding shapes for different traffic agents. Our work uses polygon representation because it is representative for most traffic agents and easy for collision checking. Some previous work has modeled human inner states. PORCA [19] infers intentions with Bayesian inference, but it assumes responsibility changes deterministically and all the traffic agents are fully attentive. The work in [20] learns a linear mapping from selected features to attention values. The mapping, however, is learned for cars and might not be suitable for traffic agents of other types.

2.2 Deep Learning Approaches For Motion Prediction

Considerable research has been done for motion prediction with deep learning approaches. S-LSTM [21] models each agent’s trajectory with one LSTM, and models their interactions using a “social pooling layer” which connects spatially proximal LSTMs to share information with each other. S-GAN [22] improves on S-LSTM by introducing generative adversarial network to it. SoPhie [23] leverages a social attention module which learns the interactions between agents, and a physical attention module which learns the physical constraints in the scene, to predict trajectories. These three works achieve high accuracy for motion prediction. However, they are designed specifically for pedestrians and are not suitable for other traffic agents such as cars. Another group of work focuses on vehicle trajectory prediction [24,25,26,27,28]. They are all based on recurrent neural network. One limitation of this group of work is again the motion prediction for only one type of traffic agents. They may not work well for heterogeneous traffic agents with different kinematics and geometry. TraPHic [29] and TrafficPredict [30] can handle heterogeneous traffic agents with different kinematics and geometry. TraPHic implicitly models dynamics and shapes by embedding dynamics- and shape-relevant features in the input state space, while TrafficPredict uses “category layers”, which learn the similarities of traffic agents of the same type, to refine the predictions of the traffic agents based on their types. All those deep learning approaches do not model human inner states explicitly. Instead, they directly model the interactions in a deep learning fashion. This often results in overfitting to the training scenes, which we will demonstrate in the experiment section. Another common issue of the deep learning approaches is the requirement of large training data; but training data is often very difficult to obtain.

Furthermore, an ultimate goal of motion prediction is to help in autonomous driving; deep learning approaches are often not computationally efficient to be integrated into a planning algorithm for autonomous driving.

3 Problem Formulation

We aim to predict the future positions of multiple traffic agents over a horizon t_{pred} , given their history positions of length t_{hist} , their agent types (e.g., cars, pedestrians, etc.), and static obstacles in the environment.

Suppose that there are N traffic agents and K obstacles in the environment. We denote the 2D positions of the i -th traffic agent at a time step t as $\mathbf{p}_t^i = (x_t^i, y_t^i)$ and its type as type^i . Obstacles are represented as a polygon, where the i -th obstacle with M vertices is represented as $o^i = \{(x_j^i, y_j^i) \mid j = 1, 2, \dots, M\}$.

At time step t , our goal is to predict the future positions of all traffic agents:

$$\mathbf{P}_{t+1:t+t_{\text{pred}}} = \{\mathbf{p}_{t+1:t+t_{\text{pred}}}^i \mid i = 1, 2, \dots, N\},$$

given their history positions $\mathbf{P}_{t-t_{\text{hist}}:t}$ and agent types

$$\mathbf{T} = \{\text{type}^i \mid i = 1, 2, \dots, N\},$$

as well as obstacles in the environment:

$$\mathbf{O} = \{o^i \mid i = 1, 2, \dots, K\}.$$

Different from previous work [1,12,13], we assume that the motion of traffic agents are conditioned on the unknown human inner states. We apply Bayesian inference to maintain a probability distribution over the human inner states, and generate multiple hypotheses of $\mathbf{P}_{t+1:t+t_{\text{pred}}}$ instead of one.

4 GAMMA

The motion of traffic agents are determined by physical constraints, such as kinematics and geometry, and human inner states such as intention, attention, and responsibility. Our motion prediction model, GAMMA, integrates both physical constraints and human inner states into a unified framework of geometric optimization. It assumes each traffic agent optimizes its velocity based on its intention while constrained by kinematics, geometry, attention, and responsibility. In the following, we will first present our optimization framework, and then introduce in detail how we incorporate different factors into the framework.

4.1 Optimization Framework

We formulate motion prediction as a constrained optimization problem. Given a group of traffic agents, we compute for each agent an instantaneous velocity close to its intended one, which is guaranteed to be collision-free for at least τ time and feasible for the traffic agent’s kinematics. We introduce the feasible space and objective function of the problem in the following.

Feasible Velocity Set For a given traffic agent, GAMMA finds a set of velocities that is *kinematically trackable* and *geometrically feasible* for the traffic agent. A velocity v is called kinematically trackable if A can track v with its low-level controller below a predefined maximum tracking error ε_{\max} for τ time. A velocity v for a traffic agent A is defined as geometrically feasible with respect to another traffic agent B if it does not lead to collisions between them supposing that A moves at v for τ time. We denote the set of kinematically trackable velocities as K_A^τ , the set of geometrically feasible velocities for agent A with respect to agent B as $G_{A|B}^\tau$. Moreover, traffic agents only has limited attention capabilities. A real-world traffic agent only react to agents within its attentive range, denoted as $\text{Att}(A)$. Hence, GAMMA finds the optimal velocity for a traffic agent A from $G_A^\tau \cap K_A^\tau$, where $G_A^\tau = \bigcap_{B \in \text{Att}(A)} G_{A|B}^\tau$.

Velocity Optimization To predict the motion of A , GAMMA computes a velocity that is closest to its *preferred velocity* v_A^{pref} derived from A ' intention. This optimization is conducted on the feasible velocity set $G_A^\tau \cap K_A^\tau$, i.e.,

$$v_A^{\text{new}} = \arg \min_{v \in G_A^\tau \cap K_A^\tau} \|v - v_A^{\text{pref}}\|. \quad (1)$$

The objective function here is quadratic. Moreover, both G_A^τ and K_A^τ are convex because of the way they are constructed (Sec. 4.2). Therefore, we can efficiently solve the optimization problem using linear programming. The actual prediction of A 's motion is generated by tracking v_A^{new} using A 's low-level controller for one time step. This process repeats for t_{pred} steps for all traffic agents at time t to predict their future positions $\mathbf{P}_{t+1:t+t_{\text{pred}}}$.

4.2 Modeling Physical Constraints and Human Inner States

GAMMA integrates both physical constraints and human inner states into the optimization framework. In this section, we will introduce the modeling of the following five factors in detail: kinematics, geometry, intention, attention, and responsibility.

Kinematics Modeling Real-world traffic agents have versatile types of kinematics. Most of vehicles are non-holonomic, meaning that they cannot move freely side-wise. To consider the influence of kinematics for traffic agents' motions, we follow the ideas in [12] and [13] to introduce additional kinematic constraints to the feasible velocity space. GAMMA only chooses from velocities that can be tracked by the agent's kinematics within a maximum tracking error ε_{\max} . The final prediction is generated by tracking the velocity output by GAMMA using a low-level controller. Noticeably, both [12] and [13] are specifically designed for one single type of kinematics. The challenge here is to model traffic agents with *heterogeneous* kinematics, such as holonomic (pedestrians), car-like (cars, bicycles, motorbikes, etc.), differential-drive (gyro-scooters), trailer-like (trucks), etc..

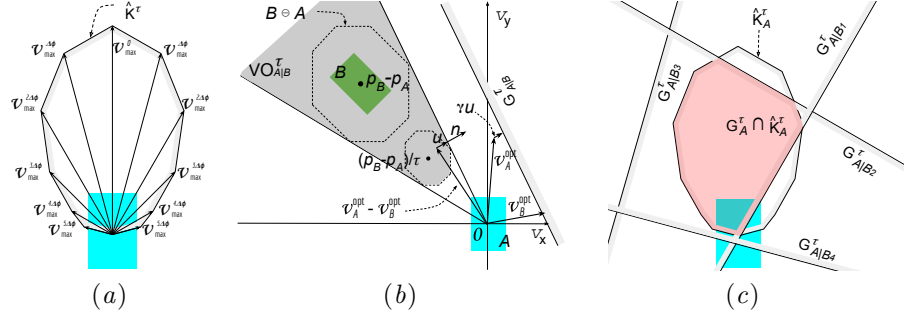


Fig. 1. (a) The estimated kinematically trackable velocity set, \hat{K}^τ , is estimated using the convex hull of $\{v_{max}^\phi \mid \phi \in \Phi\}$. (b) $VO_{A|B}^\tau$ (gray) and $G_{A|B}^\tau$ (half plane). The velocity obstacle of agent A (blue) induced by agent B (green) for time τ , is a truncated cone with its apex at the origin (in velocity space) and its legs tangent to the polygon $B \ominus A$. $G_{A|B}^\tau$ is a half-plane divided by the line that is perpendicular to the vector u through the point $v_A^{opt} + \gamma u$, where u is the vector from $v_A^{opt} - v_B^{opt}$ to the closest point on the boundary of $VO_{A|B}^\tau$. (c) An example of the feasible velocity space of a traffic agent A . The feasible space, shaded in red, is the intersection of \hat{K}_A^τ and the geometry constraints induced by four other traffic agents: $G_{A|B_1}^\tau, G_{A|B_2}^\tau, G_{A|B_3}^\tau,$ and $G_{A|B_4}^\tau$.

For a given traffic agent A , we need to find the *kinematically trackable velocity set*, K_A^τ , *s.t.*,

$$K_A^\tau = \{v \mid \|vt - f_A(v, t)\| \leq \varepsilon_{max}, \forall t \in [0, \tau]\}, \quad (2)$$

where $f_A(v, t)$ is the position of A at time t if it tracks v with its low-level controller. $f_A(v, t)$ varies for different types of kinematics and low-level controllers. It is often intractable to compute an analytic form of $f_A(v, t)$ for different kinematics and controllers. We propose to estimate K_A^τ numerically offline. We assume that the same type of traffic agents corresponds to the same kinematics and low-level controllers. Therefore, we only need to estimate K^τ 's for representative types of traffic agents: pedestrian, bicycle, motorbike, car, van, bus, gyro-scooter, trucks, etc..

For a specific type of traffic agents, we estimate its kinematically trackable velocity set K^τ by first discretizing the set of holonomic velocities $\{v\}$ and running the controller offline to measure the maximum error ε_v for tracking v . Then K^τ is estimated as the convex hull of the discretized velocities with $\varepsilon_v \leq \varepsilon_{max}$.

Concretely, we discretize v along its two dimensions (s_v, ϕ_v) , where s_v is the speed and ϕ_v is the deviation angle from traffic agent's heading direction, into two discrete sets $S = [0 : \Delta s : s_{max}]$ and $\Phi = [0 : \Delta \phi : \phi_{max}]$. This forms a discretized velocity set V :

$$v \in V = \{v \mid s_v \in S, \phi_v \in \Phi\}. \quad (3)$$

For each $v \in V$, we run the controller offline to track it for a duration of τ and record its maximum tracking error ε_v . Then we determine the velocities on

the boundary of the trackable set as follows. For each deviation angle $\phi \in \Phi$, we collect a set V_ϕ of discretized velocities with deviation angle ϕ and has a tracking error less than ε_{\max} , i.e., $V_\phi = \{v \in V \mid \phi_v = \phi, \varepsilon_v \leq \varepsilon_{\max}\}$. Then, we pick a velocity v_{\max}^ϕ from V_ϕ that has the maximum speed:

$$v_{\max}^\phi = \arg \max_{v \in V_\phi} s_v. \quad (4)$$

v_{\max}^ϕ for all ϕ 's form the boundary of the trackable velocity set, and we approximate K^τ by computing the convex hull \hat{K}^τ :

$$\hat{K}^\tau = \text{ConvexHull}(\{v_{\max}^\phi \mid \phi \in \Phi\}). \quad (5)$$

Geometrically, \hat{K}^τ is a polygon in velocity space (Fig. 1a). Approximating K^τ , of course, brings a small approximation error. However, we claim that GAMMA is robust to the approximation error.

Geometry Modeling For a given traffic agent A , we construct $G_{A|B}^\tau$, the geometrically feasible velocity set of A with respect to another traffic agent B . We extend the definitions in [1] to handle traffic agents with more general geometry. GAMMA first constructs a velocity obstacle for A with respect to B , then derives the geometrically feasible velocity set $G_{A|B}^\tau$ based on the velocity obstacle.

Consider two agents A and B at position \mathbf{p}_A and \mathbf{p}_B , respectively. The velocity obstacle $\text{VO}_{A|B}^\tau$ is defined as the set of all *relative* velocities of A with respect to B that will result in collision before time τ . The *velocity obstacle*, $\text{VO}_{A|B}^\tau$, of A induced by B with time window τ is written as:

$$\text{VO}_{A|B}^\tau = \{v \mid \exists t \in [0, \tau], t \cdot v \in (B \ominus A)\}. \quad (6)$$

where $B \ominus A$ represents the *Minkowski difference*, which essentially inflates the geometry of B by that of A , and treats A as a single point. Note that the definition of velocity obstacle in [1] assumes the geometry of traffic agents to be disc-shaped. This loose representation leads to overly conservative motions in crowded scenes, especially for traffic agents with large aspect ratios such as cars and bicycles. Instead, GAMMA adopts a polygon representation, which fits tighter with most real-world traffic agents. Fig. 1b visualizes a velocity obstacle constructed with two polygon-shaped agents.

We construct $G_{A|B}^\tau$ with respect to the *optimization velocities* of the agents (often set to their current velocities) similar to [1]. Consider the case where A and B will collide with each other before time τ by taking their optimization velocities v_A^{opt} and v_B^{opt} . To achieve collision avoidance with the least cooperative effort, GAMMA finds a relative velocity closest to $v_A^{\text{opt}} - v_B^{\text{opt}}$ from the boundary of $\text{VO}_{A|B}^\tau$. Let u be the vector from $v_A^{\text{opt}} - v_B^{\text{opt}}$ to this optimal relative velocity:

$$u = \left(\arg \min_{v \in \partial \text{VO}_{A|B}^\tau} \|v - (v_A^{\text{opt}} - v_B^{\text{opt}})\| \right) - (v_A^{\text{opt}} - v_B^{\text{opt}}). \quad (7)$$

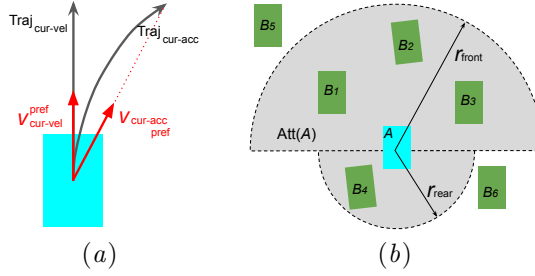


Fig. 2. (a) We represent an agent’s intention as whether it wants to keep moving at current velocity or at current acceleration. The corresponding preferred velocities, $v_{\text{cur-vel}}^{\text{pref}}$ and $v_{\text{cur-acc}}^{\text{pref}}$, have a speed equal to the agent’s current speed, and a direction pointing to the end of $\text{Traj}_{\text{cur-vel}}$ and $\text{Traj}_{\text{cur-acc}}$, the trajectories of driving at current velocity or at current acceleration for time t_{pred} , respectively. (b) $\text{Att}(A)$ (gray) with r_{front} and r_{rear} . The agent A will only react to agents inside $\text{Att}(A)$, i.e., B_1 , B_2 , B_3 , and B_4 .

So u is the smallest change on the relative velocity to avoid the collision within τ time. GAMMA lets each agent take $\gamma \in [0, 1]$ of the responsibilities for collision avoidance, i.e., adapt its velocity by (at least) $\gamma \cdot u$. Then $G_{A|B}^\tau$ is constructed as a half plane:

$$G_{A|B}^\tau = \{v \mid (v - (v_A^{\text{opt}} + \gamma \cdot u)) \cdot n \geq 0\}, \quad (8)$$

where n is the outward normal at point $(v_A^{\text{opt}} - v_B^{\text{opt}}) + u$ on the boundary of $\text{VO}_{A|B}^\tau$. A visualization of $G_{A|B}^\tau$ is shown in Fig. 1b. Note that the responsibility is an inner state of human to be inferred (Sec. 4.2).

Since $G_{A|B}^\tau$ is a half plane in the velocity space, $G_A^\tau = \bigcap_{B \in \text{Att}(A)} G_{A|B}^\tau$ is convex. Moreover, since K_A^τ is convex, the feasible velocity space $G_A^\tau \cap K_A^\tau$ will also be convex. Fig. 1c visualizes an example feasible space induced by both K_A^τ and G_A^τ considering four other traffic agents.

Intention Modeling GAMMA computes a preferred velocity v^{pref} for each agent based on its intention, and uses v^{pref} as the optimization target (Eq. 1). The intention of a traffic agent is commonly represented as navigating to a goal location, where the set of possible goals are known a priori for each environment [1,19]. This intention representation limits its application to complex real-world environments in the following aspects. First, we need to re-specify the goal positions for each new environment, which requires a lot of manual work. Second, the actual goals of traffic agents may not be covered by the predefined set, making the prediction model inaccurate in these cases. Third, since traffic agents target at a fixed goal location and GAMMA only performs local optimization, a traffic agent can be easily trapped by large obstacles blocking the goals.

We propose a new intention representation to address these issues. We define the intention of a traffic agent as whether it wants to keep moving at current velocity or at current acceleration. This design is based on two observations: 1)

constant velocity model often predicts well when a traffic agent intends to go straight, and 2) constant acceleration model often predicts well when the traffic agent intends to turn. Based on the observations, we apply Bayesian inference to infer each agent’s actual intention using its history positions. See Eq. 13 for details on the Bayesian inference. Given an inferred intention, we generate a reference position for the agent by applying the current velocity/acceleration for t_{pred} time. This reference position defines the preferred velocity v^{pref} of the traffic agent, by assigning a direction pointing to the position and a speed equal to its current speed (See Fig. 2a).

Attention Modeling Real-world traffic agents only has limited attention capabilities. An agent does not pay uniform attention to all nearby traffic agents. For instance, it reacts more to the agents in front because they are critical to collision avoidance. Different traffic agents usually have different *attentive radii*, i.e., the radius within which other agents will be paid attention to. For example, aggressive traffic agents often have smaller attentive radii, while conservative drivers often have larger attentive radii.

According to above discussions, GAMMA adopts a half-circle attention mechanism. It uses two half circles to model the attention: one in front of the vehicle with radius r_{front} , and one at the back with radius r_{rear} . We set $r_{\text{rear}} \leq r_{\text{front}}$, giving more attention to agents in the front. The actual values of r_{front} and r_{rear} are also determined using Bayesian inference (Eq. 13). Particularly, we define a small set of typical values for r_{front} and r_{rear} , and then infer for each traffic agent the most likely values using its history.

Let $\text{Att}(A)$ denote the agents inside the inferred half circles of A . GAMMA only models the interactions between A and agents in $\text{Att}(A)$. Namely, it only considers the constraints induced by a traffic agent B if B is in $\text{Att}(A)$:

$$G_A^\tau = \bigcap_{B \in \text{Att}(A)} G_{A|B}^\tau. \quad (9)$$

Fig. 2b visualizes an example of $\text{Att}(A)$ and the corresponding half circles.

Responsibility Modeling The responsibility that a traffic agent is willing to take for reciprocal collision avoidance is correlated to its agent type and the distance between the interacting agents. A vehicle interacting with a pedestrian often takes more responsibility for collision avoidance when they are far apart. But when they approximate to each other, the pedestrian will take more responsibility because it is more flexible in side-wise movements. We assume that the responsibility of a traffic agent changes linearly with its distance to other traffic agents: $\gamma = C_1 \cdot d + C_2$, where γ is the responsibility and d is the distance. The coefficient C_2 determines the initial responsibility and C_1 indicates the responsibility changing rate.

This model is similar to that in [19]. But now the coefficients, C_1 and C_2 , differ for each agent and need to be inferred. We predefined a set of values of

C_1 and C_2 for each type of traffic agents based on our thumb of rule that, the more physical constraints a traffic agent has, the larger its initial responsibility (C_2) and the smaller its responsibility changing rate (C_1) are. Then, we apply Bayesian inference (Eq. 13) to infer their actual values based on the agent’s history positions. To use the inferred responsibility value, we first normalize the value of the two agents so that they sum up to one. Then, the responsibility is injected into Eq. 8 to construct the pair-wise collision avoidance half plane. Note that GAMMA can also model static obstacles as static traffic agents by assigning them a responsibility of 0 and a preferred velocity of 0.

Bayesian Inference for Human Inner States Human inner states like intention, attention and responsibility are not observable, thus we can only infer a distribution over possible values from agents’ history positions. We apply Bayesian inference to achieve this. For each history time step, we execute GAMMA with a fixed set of human inner states to simulate the stochastic dynamics of a traffic agent and compute the likelihood of its actual movement. This is repeated for all possible combinations of inner states to get all likelihood values. Then, we apply the Bayes’ rule to incorporate the likelihood values, update the prior, and obtain a posterior distribution.

Formally, given a particular set of human inner states, denoted as:

$$\mathcal{H} = (\text{intent}, r_{\text{front}}, r_{\text{rear}}, C_1, C_2), \quad (10)$$

we provide a stochastic estimation for the next position of the agent, by executing GAMMA to get a mean position $\mathbf{p}^{\text{GAMMA}}$ and adding a Gaussian noise to it:

$$\mathbf{p}_t = \mathbf{p}_t^{\text{GAMMA}}(\mathcal{H}, \mathbf{P}_{t-t_{\text{hist}}:t-1}, \mathbf{T}, \mathbf{O}) + \epsilon, \quad \epsilon \sim \mathcal{N}(0, \sigma^2). \quad (11)$$

where $\mathbf{P}_{t-t_{\text{hist}}:t-1}$ are history positions, \mathbf{T} is the set of agent types, and \mathbf{O} is the set of static obstacles in the environment. The Gaussian noise has a predefined variance σ^2 . We assume that $\mathbf{P}_{t-t_{\text{hist}}:t-1}$, \mathbf{T} , and \mathbf{O} are fully observable because they are relatively accurate and their noises do not pose significant effect on motion prediction compared to human inner states. We also assume that a traffic agent does not change its inner state during the prediction horizon.

For an observed agent position \mathbf{p}_t at a history time step t , the observation likelihood is computed as:

$$p(\mathbf{p}_t | \mathcal{H}, \mathbf{P}_{t-t_{\text{hist}}:t-1}, \mathbf{T}, \mathbf{O}) = f(\|\mathbf{p}_t - \mathbf{p}_t^{\text{GAMMA}}\| | 0, \sigma^2). \quad (12)$$

where f is the probability density function of the normal distribution. Next, we update the probability distribution over \mathcal{H} at time step t using the Bayes’ rule:

$$p_t(\mathcal{H}) = \eta \cdot p(\mathbf{p}_t | \mathcal{H}, \mathbf{P}_{t-t_{\text{hist}}:t-1}, \mathbf{T}, \mathbf{O}) \cdot p_{t-1}(\mathcal{H}), \quad (13)$$

where $p_{t-1}(\mathcal{H})$ is the prior distribution, $p_t(\mathcal{H})$ is the posterior at time step t , and η is a normalization constant. After parsing through all history positions of an agent, we obtain an informed distribution over its inner states.

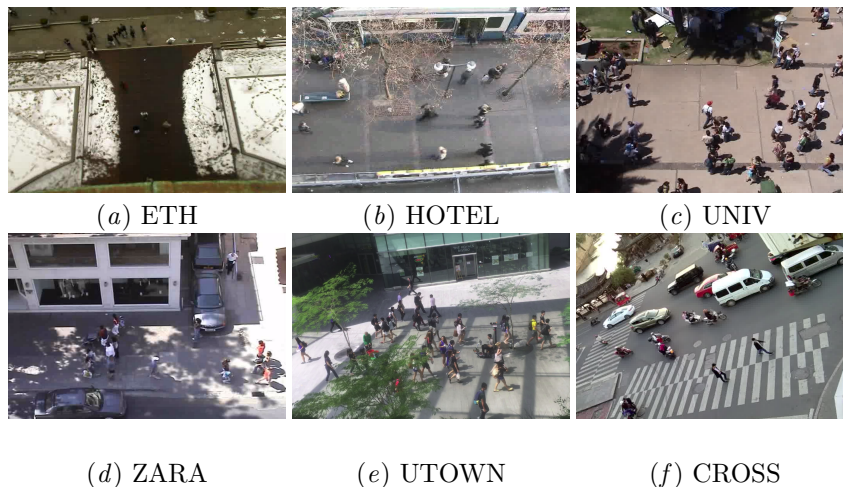


Fig. 3. Screenshots for the datasets. (a) and (b) are ETH dataset. (c) and (d) are UCY dataset. (e) UTOWN dataset. (f) CROSS dataset.

5 Experiments and Results

In this section, we evaluate our approach, GAMMA, on four datasets: ETH[31], UCY[32], UTOWN, and CROSS. We first evaluate GAMMA on *homogeneous* datasets with only pedestrians (ETH and UCY) in Sec. 5.2, and then on *heterogeneous* datasets with various types of traffic agents (UTOWN and CROSS) in Sec. 5.1. GAMMA is compared with both deep learning approaches and traditional approaches. We also conduct an ablation study in Sec. 5.3.

Datasets. ETH and UCY are standard benchmark datasets available online. ETH consists of two scenes: a plaza outside the ETH building (ETH) and a street outside a hotel (HOTEL); UCY also consists of two scenes: a university plaza (UNIV), and a street outside Zara (ZARA1 and ZARA2). However, the two datasets contain only pedestrians. To test our predictor on heterogeneous traffic agents, we further collected two datasets: UTOWN and CROSS. UTOWN presents a campus plaza where many pedestrians interacting with a vehicle scooter. CROSS presents an *unsignalized* cross scene with various types of traffic agents, including cars, vans, buses, bicycles, motorcycles, electric-tricycles, and pedestrians. See Fig. 3 for the screenshots of the dataset scenes.

Evaluation Metrics. Following prior work [26,22], we report two error metrics:

- Average Displacement Error (**ADE**). The average Euclidean distance between the predicted position and the ground-truth position over all the time frames for a prediction duration t_{pred} .

Table 1. Performance comparison across homogeneous benchmark datasets, ETH (ETH and HOTEL) and UCY (UNIV, ZARA1, and ZARA2), where traffic agents are all pedestrians. We report ADE and FDE for a prediction time $t_{\text{pred}} = 12$ steps (4.8 seconds) in meters. We use a history of $t_{\text{hist}} = 3$ steps (1.2 seconds) for inferring the human inner states. We also report their average values (AVG) over all the datasets.

Metric	Dataset	LR	LSTM	S-LSTM	S-GAN	PORCA	GAMMA
ADE/FDE	ETH	1.33/2.94	1.09/2.41	1.09/2.35	0.81/ 1.52	0.78/1.81	0.77/1.80
	HOTEL	0.39/0.72	0.86/1.91	0.79/1.76	0.72/1.61	0.34/0.74	0.30/0.65
	UNIV	0.82/1.59	0.61/1.31	0.67/1.40	0.60/1.26	0.45/1.11	0.42/1.03
	ZARA1	0.62/1.21	0.41/0.88	0.47/1.00	0.34/ 0.69	0.34/0.83	0.33/0.82
	ZARA2	0.77/1.48	0.52/1.11	0.56/1.17	0.42/0.84	0.34/0.85	0.27/0.66
AVG		0.79/1.59	0.70/1.52	0.72/1.54	0.58/1.18	0.45/1.07	0.42/0.99

- Final Displacement Error (**FDE**). The Euclidean distance between the predicted position and the ground-truth position at the final time frame for a prediction duration t_{pred} .

Note that GAMMA generates multiple trajectories for each traffic agent corresponding to its multiple possible human inner states. Each trajectory has a probability equal to that of its corresponding human inner state (Eq. 13). For a realistic comparison, we report the ADE and FDE for GAMMA using the trajectory with the maximum probability instead of using the one that best matches the ground-truth. One of our baselines, S-GAN, reports the results using the best-matched trajectory from 20 samples. Nevertheless, GAMMA still significantly outperform S-GAN (see Sec. 5.1).

5.1 Evaluation on Homogeneous Datasets

We compare GAMMA with both state-of-the-art deep learning approaches and state-of-the-art traditional approach on homogeneous benchmark datasets, ETH and UCY, which only contain pedestrians. The baselines include,

- LR: A linear regressor minimizing least square error over history trajectories.
- LSTM: A vanilla recurrent neural network with LSTM cells.
- S-LSTM: Social LSTM proposed in [21], which models each trajectory with one LSTM, and models their interactions using a social pooling layer.
- S-GAN: Social GAN proposed in [22], which introduces generative adversarial network into S-LSTM to improve performance.
- PORCA: State-of-the-art approach proposed in [19]. PORCA is a geometric optimization based approach similar to GAMMA, but it does not consider the heterogeneous kinematics and geometry.

The ADE and FDE of GAMMA and the baselines are shown in Table 1. GAMMA outperforms all the baselines, especially, the state-of-the-art approaches, S-GAN and PORCA, in almost all datasets.

GAMMA significantly beats the deep learning approaches: LR, LSTM, S-LSTM and S-GAN. One interesting finding is that, both GAMMA and LR significantly outperform the other deep learning baselines in the HOTEL scene, which

Table 2. Performance comparison across CROSS and UTOWN datasets, where various types of traffic agents are interacting with each other. We report ADE and FDE for a prediction time $t_{\text{pred}} = 15$ steps (5 seconds) in meters. We use a history of $t_{\text{hist}} = 3$ steps (1 second) for inferring the human inner states. We also report their average values (AVG) over the two datasets.

Metric	Dataset	CONST-VEL	PREF-VEL	PORCA	GAMMA
ADE/FDE	CROSS	1.39/3.49	1.31/2.98	1.42/3.50	1.15/2.77
	UTOWN	1.04/2.12	0.95/1.92	0.93/1.89	0.85/1.61
AVG		1.22/2.80	1.13/2.45	1.18/2.63	1.00/2.19

Table 3. ADE/FDE comparison on the split CROSS dataset for a prediction time $t_{\text{pred}} = 15$ steps (5 seconds) in meters. We use a history of $t_{\text{hist}} = 3$ steps (1 second) for inferring the human inner states. CROSS dataset is split into CROSS_{straight} containing straight-line trajectories, and CROSS_{turn} containing curving trajectories.

Metric	Dataset	CONST-VEL	PREF-VEL	PORCA	GAMMA
ADE/FDE	CROSS _{straight}	1.38/3.42	1.30/3.00	1.40/3.43	1.18/2.75
	CROSS _{turn}	1.46/3.85	1.37/2.84	1.52/3.87	1.00/2.84

is less crowded and mostly contains straight-line trajectories. LSTM, S-LSTM and S-GAN perform much worse than LR in this less complex scene, demonstrating that the complex models might overfit to the more complex scenes. In contrast, our approach performs well in both simple and complex scenes.

GAMMA also beats a very strong traditional approach, PORCA, in all homogeneous benchmark datasets. Although the performance gain is not as significant as those corresponding to the deep learning approaches, we claim that PORCA cannot predict well for heterogeneous traffic agents and GAMMA can outperform PORCA very significantly on datasets with heterogeneous traffic agents. We demonstrate this statement in the next section.

5.2 Evaluation on Heterogeneous Datasets

We evaluate our method, GAMMA, on the UTOWN and CROSS datasets, which contain various types of traffic agents such as pedestrians, cars, bicycles, and buses. We compare GAMMA with several baselines. Since the aforementioned deep learning approaches, LR, LSTM, S-LSTM and S-GAN, are specifically designed for predicting pedestrian motions, we do not add them as baselines for predicting motions of heterogeneous traffic agents. Instead, we add two more traditional approaches together with PORCA as the baselines:

- CONST-VEL: A model assuming that each traffic agent will keep moving at its current velocity.
- PREF-VEL: A model assuming that each traffic agent will keep moving at its preferred velocity. The preferred velocity is set to the one inferred in GAMMA, i.e., the target velocity v^{pref} in Eq. 1.
- PORCA: As described in Sec. 5.2.

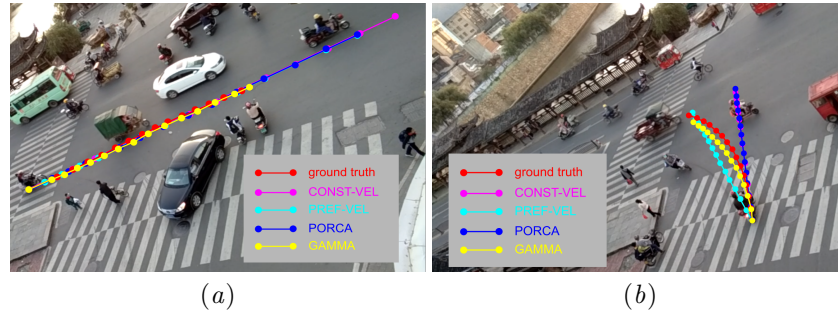


Fig. 4. The trajectory predictions of different algorithms compared with the ground truth. (a) For a straight-line trajectory, GAMMA successfully predicts that the scooter will drive at a low speed because of the vehicles in front, while the other algorithms fail to do so. (b) For a curving trajectory, GAMMA successfully predicts a curving trajectory while the other algorithms predict straight-line trajectories.

We show the ADE and FDE for all algorithms in Table 2. Clearly, GAMMA outperforms all the baselines, especially for the challenging CROSS dataset, where various types of traffic agents move in a highly interactive manner. See <https://youtu.be/5xAB0-8XceQ> for a video of prediction on CROSS dataset.

To investigate the performance gain, we further split the CROSS dataset into two sub-datasets, $CROSS_{\text{straight}}$ and $CROSS_{\text{turn}}$. $CROSS_{\text{straight}}$ contains trajectories that drive nearly in straight lines, while $CROSS_{\text{turn}}$ contains trajectories that make turns. The ADE and FDE of all the algorithms are shown in Table 3. GAMMA achieves a much higher prediction accuracy on $CROSS_{\text{turn}}$. This is because only GAMMA takes into account kinematics. Other algorithms all incorrectly predict straight-line trajectories for $CROSS_{\text{turn}}$ since no kinematic constraints are considered.

We further select two example scenes in CROSS and visualize the predictions in Fig. 4. Fig. 4a explains GAMMA’s performance improvement for straight-line trajectories. Although all the algorithms correctly predict the trajectory directions, only GAMMA successfully predicts that the scooter will drive at a low speed to avoid collisions. CONST-VEL and PREF-VEL fail to do so because they assume traffic agents will not react to each other. PORCA also fails to slow down the traffic agents because it imposes no kinematic constraints on them, thinking that they can flexibly avoid collisions even when they get close to each other. Fig. 4b explains GAMMA’s performance improvement for turning trajectories. Only GAMMA successfully predicts a curving trajectory to the goal because only it takes into account the kinematics.

5.3 Ablation Study

To study the importance of the five components of the motion model, we conduct an ablation study. We test GAMMA in the absence of each component while holding the other components constant. For GAMMA w/o kinematic constraints,

Table 4. Ablation study for GAMMA on the CROSS dataset. ADE and FDE are reported for the prediction time $t_{\text{pred}} = 15$ steps (5 seconds) in meters. We use a history of $t_{\text{hist}} = 3$ steps (1 second) for inferring the human inner states.

Metric	GAMMA w/o kinematic constraints	GAMMA w/o tight geometry representation	GAMMA w/o intention inference	GAMMA w/o attention inference	GAMMA w/o responsibility inference	GAMMA
ADE/FDE	1.42/3.47	1.37/3.22	1.47/3.25	1.16/2.78	1.16/2.77	1.15/2.77

we set all traffic agents to be holonomic. For GAMMA w/o tight geometry representation, we set all traffic agents to be disc-shaped. For GAMMA w/o intention inference, we set the intention of all the traffic agents to keeping moving at current velocity. For GAMMA w/o attention inference, we set the attention of all the traffic agents to be 1. For GAMMA w/o responsibility inference, we set the responsibility of all the traffic agents to be 0.5. We select CROSS as the testing dataset. The results are presented in Table 4. As we can see, each of the five components contributes to the performance gain of GAMMA. Kinematic constraints, tight geometry representation, and intention inference play a more important role in improving the model.

6 Conclusions and Future Work

We developed GAMMA, a general motion prediction model that models heterogeneous traffic agents with different physical constraints and human inner states. We proposed a unified framework of geometric optimization that incorporates key factors for motion prediction including kinematics, geometry, intention, attention, and responsibility. Experimental results show that GAMMA significantly outperforms both geometry-based and deep learning approaches on various real-world datasets.

Currently, we only used simple models for intention, attention, and responsibility. In the future, we plan to investigate more sophisticated intention representations and models for attention and responsibility in order to handle complex scenarios. Note that the GAMMA framework can be easily extended to incorporate more factors, such as courtesy, patience, social comfort zones, etc..

References

1. J. Van Den Berg, S. Guy, M. Lin, and D. Manocha, “Reciprocal n-body collision avoidance,” in *Proc. Int. Symp. on Robotics Research*, 2009.
2. D. Helbing and P. Molnar, “Social force model for pedestrian dynamics,” *Physical review E*, vol. 51, p. 4282, 1995.
3. R. Löhner, “On the modeling of pedestrian motion,” *Applied Mathematical Modelling*, vol. 34, pp. 366–382, 2010.
4. G. Ferrer, A. Garrell, and A. Sanfeliu, “Robot companion: A social-force based approach with human awareness-navigation in crowded environments,” in *Proc. IEEE/RSJ Int. Conf. on Intelligent Robots & Systems*, 2013.

5. S. Pellegrini, A. Ess, K. Schindler, and L. Van Gool, "You'll never walk alone: Modeling social behavior for multi-target tracking," in *Computer Vision, 2009 IEEE 12th International Conference on*, pp. 261–268, IEEE, 2009.
6. P. Fiorini and Z. Shiller, "Motion planning in dynamic environments using velocity obstacles," *Int. J. Robotics Research*, vol. 17, pp. 760–772, 1998.
7. J. Van den Berg, M. Lin, and D. Manocha, "Reciprocal velocity obstacles for real-time multi-agent navigation," in *Proc. IEEE Int. Conf. on Robotics & Automation*, 2008.
8. J. Snape, J. Van Den Berg, S. J. Guy, and D. Manocha, "The hybrid reciprocal velocity obstacle," *IEEE Transactions on Robotics*, vol. 27, pp. 696–706, 2011.
9. N. Deo, A. Rangesh, and M. M. Trivedi, "How would surround vehicles move? a unified framework for maneuver classification and motion prediction," *IEEE Trans. on Intelligent Vehicles*, vol. 3, no. 2, pp. 129–140, 2018.
10. A. Houenou, P. Bonnifait, V. Cherfaoui, and W. Yao, "Vehicle trajectory prediction based on motion model and maneuver recognition," in *Proc. IEEE/RSJ Int. Conf. on Intelligent Robots & Systems*, pp. 4363–4369, IEEE, 2013.
11. M. Schreier, V. Willert, and J. Adamy, "Bayesian, maneuver-based, long-term trajectory prediction and criticality assessment for driver assistance systems," in *17th Int. IEEE Conf. on Intelligent Transportation Systems*, pp. 334–341, IEEE, 2014.
12. J. Alonso-Mora, A. Breitenmoser, M. Rufli, P. Beardsley, and R. Siegwart, "Optimal reciprocal collision avoidance for multiple non-holonomic robots," in *Distributed Autonomous Robotic Systems*, pp. 203–216, Springer, 2013.
13. J. Alonso-Mora, A. Breitenmoser, P. Beardsley, and R. Siegwart, "Reciprocal collision avoidance for multiple car-like robots," in *Proc. IEEE Int. Conf. on Robotics & Automation*, 2012.
14. J. Van Den Berg, J. Snape, S. J. Guy, and D. Manocha, "Reciprocal collision avoidance with acceleration-velocity obstacles," in *Proc. IEEE Int. Conf. on Robotics & Automation*, pp. 3475–3482, IEEE, 2011.
15. D. Wilkie, J. Van Den Berg, and D. Manocha, "Generalized velocity obstacles," in *Proc. IEEE/RSJ Int. Conf. on Intelligent Robots & Systems*, pp. 5573–5578, IEEE, 2009.
16. A. Best, S. Narang, and D. Manocha, "Real-time reciprocal collision avoidance with elliptical agents," in *Proc. IEEE Int. Conf. on Robotics & Automation*, pp. 298–305, IEEE, 2016.
17. S. A. Stüvel, N. Magnenat-Thalmann, D. Thalmann, A. F. van der Stappen, and A. Egges, "Torso crowds," *IEEE Trans. on Visualization and Computer Graphics*, vol. 23, no. 7, pp. 1823–1837, 2017.
18. Y. Ma, D. Manocha, and W. Wang, "Efficient reciprocal collision avoidance between heterogeneous agents using ctmat," *Proc. of the 17th Int. Conf. on Autonomous Agents and Multiagent Systems*, 2018.
19. Y. Luo, P. Cai, A. Bera, D. Hsu, W. S. Lee, and D. Manocha, "PORCA: Modeling and planning for autonomous driving among many pedestrians," *IEEE Robotics and Automation Letters*, vol. 3, no. 4, pp. 3418–3425, 2018.
20. E. Cheung, A. Bera, and D. Manocha, "Efficient and safe vehicle navigation based on driver behavior classification," in *Proc. IEEE Conf. on Computer Vision & Pattern Recognition*, pp. 1024–1031, 2018.
21. A. Alahi, K. Goel, V. Ramanathan, A. Robicquet, L. Fei-Fei, and S. Savarese, "Social LSTM: Human trajectory prediction in crowded spaces," in *Proc. IEEE Conf. on Computer Vision & Pattern Recognition*, pp. 961–971, 2016.

22. A. Gupta, J. Johnson, L. Fei-Fei, S. Savarese, and A. Alahi, "Social GAN: Socially acceptable trajectories with generative adversarial networks," in *Proc. IEEE Conf. on Computer Vision & Pattern Recognition*, pp. 2255–2264, 2018.
23. A. Sadeghian, V. Kosaraju, A. Sadeghian, N. Hirose, and S. Savarese, "SoPhie: An attentive gan for predicting paths compliant to social and physical constraints," *arXiv preprint arXiv:1806.01482*, 2018.
24. F. Alché and A. de La Fortelle, "An LSTM network for highway trajectory prediction," in *20th Int. IEEE Conf. on Intelligent Transportation Systems*, pp. 353–359, IEEE, 2017.
25. N. Deo and M. M. Trivedi, "Convolutional social pooling for vehicle trajectory prediction," in *Proceedings of the IEEE Conference on Computer Vision and Pattern Recognition Workshops*, pp. 1468–1476, 2018.
26. N. Lee, W. Choi, P. Vernaza, C. B. Choy, P. H. Torr, and M. Chandraker, "DESIRE: Distant future prediction in dynamic scenes with interacting agents," in *Proceedings of the IEEE Conference on Computer Vision and Pattern Recognition*, pp. 336–345, 2017.
27. B. Kim, C. M. Kang, J. Kim, S. H. Lee, C. C. Chung, and J. W. Choi, "Probabilistic vehicle trajectory prediction over occupancy grid map via recurrent neural network," in *20th IEEE Int. Conf. on Intelligent Transportation Systems*, pp. 399–404, IEEE, 2017.
28. N. Deo and M. M. Trivedi, "Multi-modal trajectory prediction of surrounding vehicles with maneuver based lstms," in *IEEE Intelligent Vehicles Symp.*, pp. 1179–1184, IEEE, 2018.
29. R. Chandra, U. Bhattacharya, A. Bera, and D. Manocha, "TraPHic: Trajectory prediction in dense and heterogeneous traffic using weighted interactions," *arXiv preprint arXiv:1812.04767*, 2018.
30. Y. Ma, X. Zhu, S. Zhang, R. Yang, W. Wang, and D. Manocha, "TrafficPredict: Trajectory prediction for heterogeneous traffic-agents," in *Proc. AAAI Conf. on Artificial Intelligence*, 2019.
31. S. Pellegrini, A. Ess, and L. Van Gool, "Improving data association by joint modeling of pedestrian trajectories and groupings," in *Proc. European Conf. on Computer Vision*, pp. 452–465, Springer, 2010.
32. L. Leal-Taixé, M. Fenzi, A. Kuznetsova, B. Rosenhahn, and S. Savarese, "Learning an image-based motion context for multiple people tracking," in *Proc. IEEE Conf. on Computer Vision & Pattern Recognition*, pp. 3542–3549, 2014.